Elsevier Editorial System(tm) for Nuclear Inst. and Methods in Physics Research, A
Manuscript Draft

Manuscript Number:

Title: Present Limits on the Precision of SM Predictions for Jet Energies

Article Type: Technical Note

Section/Category: Numerical and Data Analysis

Keywords: Jet Energy Scale; JES; Collider Detector at Fermilab; CDF;
Fermilab; Parton Shower; Final State Radiation; FSR

Corresponding Author: Alexander Paramonov,

Corresponding Author's Institution: The University of Chicago

First Author: Alexander A Paramonov, PhD

Order of Authors: Alexander A Paramonov, PhD; Florencia Canelli, PhD; Monica D'Onofrio, PhD; Henry J Frisch, PhD; Stephen Mrenna, PhD

Abstract: We investigate the impact of theoretical uncertainties on the accuracy of measurements involving hadronic jets. The analysis is performed using events with a Z boson and a single jet observed in $p\bar{p}$ collisions at $\sqrt{s}$ = 1.96 TeV in \lum~of data from the Collider Detector at Fermilab (CDF). The transverse momenta (\pt) of the jet and the boson should balance each other due to momentum conservation in the plane transverse to the direction of the p and $\bar{p}$ beams. We evaluate the dependence of the measured \pt-balance on theoretical uncertainties associated with initial and final state radiation, choice of renormalization and factorization scales, parton distribution functions, jet-parton matching, calculations of matrix elements, and parton showering. We find that the uncertainty caused by parton showering at large angles is the largest amongst the listed uncertainties. The proposed method can be re-applied at the LHC experiments to investigate and evaluate the uncertainties on the predicted jet energies. The distributions produced at the CDF environment are intended for comparison to those from modern event generators and new tunes of parton showering. The comparison will allow higher accuracy of the predicted jet energies, and thus an improved discovery potential in signatures containing jets, at the LHC.

Present Limits on the Precision of SM Predictions for Jet Energies

A.A. Paramonov[a,*], F. Canelli[b], M. D'Onofrio[c], H.J. Frisch[b], S. Mrenna[d]

[a] *Argonne National Laboratory, Argonne, IL 60439, USA*
[b] *Enrico Fermi Institute, University of Chicago, Chicago, IL 60637, USA*
[c] *University of Liverpool, Liverpool L69 7ZE, UK*
[d] *Fermi National Accelerator Laboratory, Batavia, IL 60510, USA*

Abstract

We investigate the impact of theoretical uncertainties on the accuracy of measurements involving hadronic jets. The analysis is performed using events with a Z boson and a single jet observed in $p\bar{p}$ collisions at $\sqrt{s} = 1.96$ TeV in 4.6 fb^{-1} of data from the Collider Detector at Fermilab (CDF). The transverse momenta ($\mathrm{p_T}$) of the jet and the boson should balance each other due to momentum conservation in the plane transverse to the direction of the p and $\bar{p}$ beams. We evaluate the dependence of the measured $\mathrm{p_T}$-balance on theoretical uncertainties associated with initial and final state radiation, choice of renormalization and factorization scales, parton distribution functions, jet-parton matching, calculations of matrix elements, and parton showering. We find that the uncertainty caused by parton showering at large angles is the largest amongst the listed uncertainties. The proposed method can be re-applied at the LHC experiments to investigate and evaluate the uncertainties on the predicted jet energies. The distributions produced at the CDF environment are intended for comparison to those from modern event generators and new tunes of parton showering. The comparison will allow higher accuracy of the predicted jet energies, and thus an improved discovery potential in signatures containing jets, at the LHC.

Keywords: Jet Energy Scale, JES, Collider Detector at Fermilab, CDF, Fermilab, Parton Shower, Final State Radiation, FSR

1. Introduction and physics motivation

The discovery potential of LHC experiments will strongly depend on the accuracy of standard model (SM) predictions for processes containing hadronic jets [1], as the first step in establishing "new physics" has to be identifying an incontrovertible deviation from SM phenomena. The uncertainties on predictions for SM processes directly impact measurements of jet spectra, searches for new heavy particles using jet energies for kinematic reconstruction, and the calculation of missing transverse momentum, to name several

*Corresponding author
Email address: alexander.paramonov@cern.ch (A.A. Paramonov)

prevalent analysis strategies as examples. The discovery potential for supersymmetry and other models of physics beyond the SM thus relies on having calibrated methods for measuring jet energies.

It has been common practice to normalize the clustered jet energy, measured with calorimeters, to the energy of the particle jet or the parent parton [2, 3]. The correction factor is often called the jet energy scale (JES). At CDF jets are observed in non-compensating sampling calorimeters, which have a non-linear response to single particles. The simulated calorimeter response for single hadrons is tuned to match that in data [2]. The measured jet energy is corrected for instrumental effects such as the non-linear response of the calorimeters as well as for parton radiation and hadronization effects. The correction for radiation and hadronization effects is independent of the experimental setup. In addition, the jet energies are corrected for multiple $p\overline{p}$ interactions in the same bunch crossing.

The systematic uncertainties on the JES and the related measurements arise from the accuracy of the detector simulation and limitations of the methods used by SM event generators. The event generators, such as PYTHIA and ALPGEN [4, 5], use a simplified modeling of complex SM processes that can be altered by tuning internal parameters. The model-dependent aspects we investigate are the following:

- parton distribution functions (PDFs) of the colliding p and $\bar{p}$
- leading order (LO) matrix elements of tree-level processes such as $q\bar{q} \to Zg$ and $qg \to Zq$
- the parton-jet matching scheme [6]
- final state radiation (FSR)
- initial state radiation (ISR)
- the renormalization and factorization scales
- residual effects due to multiple $p\overline{p}$ interactions
- the ability of the leading-log parton showering model to describe radiation at large angles

To perform the analysis we select events with a Z boson and a jet observed in 4.6 fb^{-1} of data from CDF. A Z boson is clearly identified as a pair of opposite-sign electrons or muons with an invariant mass close to the Z-boson mass. The transverse momentum of the boson is measured with high precision so that the Z+jet sample is ideal for the analysis. We use the $\mathrm{p_T}$-balance in the event with the mean-value of the ratio $\mathrm{p_T}(jet)/\mathrm{p_T}(Z)$ as the observable of interest, to test the simulated SM predictions.

The determination of the jet energy scale used in previously-published CDF analyses was performed with about 300 pb^{-1} of data [2]. The overall uncertainty on the JES was compared to the difference in $\mathrm{p_T}$-balance between data and MC predictions for a photon-jet and a Z-jet samples; the difference in $\mathrm{p_T}$-balance was calculated in a similar fashion to the method used in the current analysis. Having significantly more

data (4.6 fb^{-1}) we investigate the systematic uncertainties affecting measurements of jet energies. Using the additional statistical power, we can disentangle the different effects contributing to the uncertainties by correlating the limitations in theoretical predictions with uncertainties on the JES.

The outline of the paper is as follows. The CDF II detector is described in Section 2. Details for MC event generators are presented in Section 3. Event selection follows in Sections 4 and 5. We show $\mathrm{p_T}$-balance in data and PYTHIA as a function of $\mathrm{p_T}(Z)$ in Section 6. In the same section we further validate LO predictions from PYTHIA and ALPGEN by checking that the relative contributions from $qg \to Zq$ and $q\bar{q} \to Zg$ diagrams are accurately modeled. Computation-related uncertainties such those due to the choice of factorization and renormalization scales are evaluated in Sections 8, 9, 10, 7, and 12. We use data to evaluate uncertainties due to mis-modeling of parton radiation at large angles and multiple $p\overline{p}$ interactions in Sections 11 and 13, respectively. The uncertainty due to detector simulations is calculated in Section 14. In Section 15 we summarize the observed uncertainties and compare those to the difference in $\mathrm{p_T}$-balance between data and the MC predictions. We present conclusions in Section 16.

2. The CDF II detector

The CDF II detector is a cylindrically symmetric spectrometer designed to study $p\overline{p}$ collisions at the Fermilab Tevatron. The detector has been extensively described in the literature [7]. Here we briefly describe the detector subsystems relevant for the analysis.

Tracking systems are used to measure the momenta of charged particles, and to trigger on and identify leptons with large transverse momentum, $\mathrm{p_T}$ [8]. A multi-layer system of silicon strip detectors (SVX) [9], which identifies tracks in both the $r-\phi$ and $r-z$ views [10], and the central outer tracker (COT) [11] are contained in a superconducting solenoid that generates a magnetic field of 1.4 T. The COT is a 3.1 m long open-cell drift chamber that makes up to 96 measurements along the track of each charged particle in the region $|\eta| < 1$. Sense wires are arranged in 8 alternating axial and stereo ($\pm 2^\circ$) super-layers with 12 wires each. For high momentum tracks, the COT $\mathrm{p_T}$ resolution is $\sigma_{\mathrm{p_T}}/\mathrm{p_T^2} \simeq 0.0017$ (GeV/c)$^{-1}$ [12].

Segmented calorimeters with towers arranged in a projective geometry, each tower consisting of an electromagnetic and a hadronic compartment [13, 14], cover the central region, $|\eta| < 1$ (CEM/CHA), and the forward region [15], $1 < |\eta| < 3.6$ (PEM/PHA). In both the central and forward regions, systems with finer spatial resolution are used to make profile measurements of electromagnetic showers at shower maximum [16] for electron identification (the CES and PES systems, respectively). Electrons are reconstructed in the CEM with an E_T [8] resolution of $\sigma(E_\mathrm{T})/E_\mathrm{T} \simeq 13.5\%/\sqrt{E_\mathrm{T}/\mathrm{GeV}} \oplus 2\%$ [13] and in the PEM with an E_T resolution of $\sigma(E_\mathrm{T})/E_\mathrm{T} \simeq 16.0\%/\sqrt{E_\mathrm{T}/\mathrm{GeV}} \oplus 1\%$ [17]. Jets are identified using a cone clustering algorithm in $\eta-\phi$ space, with cone radius $R = \sqrt{\Delta\eta^2 + \Delta\phi^2}$, as a group of electromagnetic and hadronic calorimeter towers. The CDF hadronic calorimeters have a steel-scintillator sampling design and the electromagnetic

calorimeters are built from lead and scintillator. The sampling calorimeters have a non-linear response to stable hadrons [2], which carry most of the jet momentum.

Muons are identified using the central CMU, CMP, and CMX [18, 19] muon systems, which cover the kinematic region $|\eta| < 1$. The CMU system uses four layers of planar drift chambers to detect muons with $p_T > 1.4$ GeV/c in the central region of $|\eta| < 0.6$. The CMP system consists of an additional four layers of planar drift chambers located behind 0.6 m of steel outside the magnetic return yoke, and detects muons with $p_T > 2.0$ GeV/c. The CMX detects muons in the region $0.6 < |\eta| < 1.0$ with four to eight layers of drift chambers, depending on the polar angle.

The beam luminosity is measured using two sets of gas Cherenkov counters, located in the region $3.7 < |\eta| < 4.7$. The total uncertainty on the luminosity is estimated to be 5.9%, where 4.4% comes from the acceptance and operation of the luminosity monitor and 4.0% from the calculation of the inelastic $p\overline{p}$ cross-section [20].

A 3-level trigger system [7] selects events for further analysis offline. The first two levels of triggers consist of dedicated fast digital electronics analyzing a subset of the full detector data. The third level, applied to the full data from the detector for those events passing the first two levels, consists of a farm of computers that reconstruct the data and apply selection criteria for (typically) several hundred distinct triggers.

3. Standard model predictions for events with a Z boson and jets

The standard model expectations for inclusive production of Z bosons are calculated from Monte Carlo simulations using PYTHIA and ALPGEN. Events from the two MC generators are processed through the full detector simulation to be reconstructed and analyzed like data.

The datasets for the Z + light jets signatures are produced using v6.216 of PYTHIA in which the p_T spectrum of the Z bosons, p_T^Z, has been tuned to CDF Run I data for $0 < p_T^Z < 20$ GeV/c [21], and which incorporates a tuned underlying-event, Tune AW [22]. The event generator was set to inclusive production of Z-bosons with a $M(\gamma^*/Z) > 30$ GeV/c^2 cut. Historically, a di-jet sample simulated with PYTHIA was used to determine the JES at CDF; in this study we take the Z + jets events from PYTHIA as our default benchmark sample.

Additional Z + jets samples are produced with v2.10-prime of ALPGEN that has built-in matching of the number of jets from parton showering and matrix-element production [6]. The exclusive Z + N partons (N=0,..,4) samples were combined into one inclusive sample using the corresponding cross-sections provided by ALPGEN. Showering and hadronization of jets is done with PYTHIA v6.326, Tune AW [22]. The jet-parton matching is performed at $p_T$of 15 GeV/c (referred to as matching scale) using JETCLU clustering algorithm with radius of R=0.4.

Production of Z+jet events is performed differently by stand-alone PYTHIA and ALPGEN+PYTHIA. The ALPGEN+PYTHIA calculation begins with the exact matrix elements from ALPGEN for Z+N partons (N=0,..,4), which are then interfaced with PYTHIA parton showering. The interface contains a veto algorithm that removes double-counting between matrix element and parton shower partons [6]. The stand-alone PYTHIA calculation begins with the simplest matrix element (Z+0 partons) and adds additional partons from the shower with no need for a veto. However, the first parton emission is corrected to reproduce the Z+1 parton matrix element. Thus, any substantial differences between the predictions of the two calculations (if they exist) should arise for the second jet. Both event generators use the same PDF set, CTEQ5L, and Lund string hadronization model as implemented in Pythia.

The parton showering (PS) inside the jet cone (see Section 5.1) has been extensively studied [23–25] and is in good agreement with predictions. In addition, the momentum spectra of charged-particle tracks in jets are found to be in good agreement with SM predictions [2].

The large-angle (outside of cone R=0.4) parton radiation is not described well by stand-alone parton showering model in PYTHIA; the rate of softer jets collinear to a jet is not described (e.g. see Fig. 3 in [26], distribution of $\Delta R(j2, j3)$ observed in multi-jet events). Radiation of the 3rd jet in multi-jet events is qualitatively equivalent to radiation of the 2nd jet in Z+jets events. The same issue affects the invariant mass calculated for a pair of jets, energy of a jet, and missing transverse momentum. The problem related to the parton radiation at large angles can be addressed by using an exact matrix element for multi-jet events as it is done in ALPGEN+PYTHIA simulation. The ME correction is introduced for radiated jets with p_T above the matching scale (15 GeV/c); softer radiation is produced via the same leading-log PS mechanism.

4. Description of data samples

The analysis uses events that contain either an electron with $E_T > 18$ GeV or a muon with $p_T > 18$ GeV/c selected within the central region of the detector, $|\eta| < 1$, by the trigger system. The electron dataset contains 229M events; the muon dataset contains about 65M events. The integrated luminosity of each dataset is 4.6 fb^{-1}.

5. Event selection

Both the observed and the simulated events (see Section 3) use the same selection criteria to identify electrons, muons, Z bosons, and jets. Details of the selection criteria for electrons and muons are provided in Appendix A.

5.1. Jet identification

Jets are reconstructed using JETCLU, the standard CDF cone-based clustering algorithm, with cone radii of R = 0.4, 0.7, and 1.0 [27]. The clustering is performed using calorimeter towers with raw (uncorrected)

energy above 1 GeV to form a cluster of at least 3 GeV. To resolve ambiguities with overlapping cones, cones sharing an energy fraction of more than 0.75 are merged into a single jet; otherwise the shared towers are assigned to the closest jet.

The jet energies are corrected for the non-uniformity in η of the calorimeters response and for the multiple $p\overline{p}$ interactions. In this analysis, the leading jet energy is always corrected to the parton level; the jet energy scale is adjusted to relate the measured energy of a simulated jet and the energy of the corresponding parton in di-jet events [2] from PYTHIA. The jet clustering algorithm is run over calorimeter towers for reconstructed jets, over stable particles for hadron-level jets. The correction from the hadron to the parton level is a function of only jet $\mathrm{p_T}$ and is the same for data and predictions.

Calorimeter clusters that coincide with an identified electron, or photon are removed from the jet collection to avoid ambiguities. High-$\mathrm{p_T}$ photons are not rare in hard-scattering events. Identifying photons as jets and then correcting them as jets can lead to mis-measured $\mathrm{p_T}$-balance. To avoid photon misidentifications the event selection requires the leading jet to have EM-fraction less than 0.95. The EM-fraction is the fraction of energy of a jet deposited in the electromagnetic compartment of the calorimeter in comparison to the total energy of the jet.

5.2. Reconstruction of Z + jet events

Pairs of oppositely-charged electrons and muons are identified as Z-boson candidates if the reconstructed invariant mass falls in the mass window from 80 GeV/c^2 to 100 GeV/c^2. The selection of $Z \to \ell\ell$ events requires two tight leptons or a tight and a loose lepton (see Appendix A). The two leptons are required to be assigned to the same primary vertex which z-coordinate is required to be within 60 cm from the CDF center of coordinates. Also we remove dimuon events where the leading jet coincides with one of the muons forming a Z boson. Figure 1 shows the distributions in invariant mass for electron and muon pairs; the data are in a remarkable agreement with SM predictions from PYTHIA and ALPGEN.

Events are further required to have at least one jet. First, we correct all jet energies for η-dependent response of the calorimeters and for multiple $p\overline{p}$ interactions; the leading jet $\mathrm{p_T}$ is required to be greater than 8 GeV/c. An event is vetoed if the second jet cluster, sub-leading jet, has $\mathrm{p_T}$ of more than 8 GeV/c. The leading jet's absolute value of detector η is required to be from 0.2 up to 0.8, $0.2 < |\eta_{\mathrm{det.}}| < 0.8$, to avoid cracks in the central calorimeter. We do not apply the η requirement to sub-leading jets; their pseudo-rapidity can be from -2.8 to 2.8. Then the momentum of the leading jet is corrected to the parton level as described above (see Sec. 5.1). The $\vec{\mathrm{p}}_{\mathrm{T}}$ of the leading jet, $\vec{\mathrm{p}}_{\mathrm{T}}(jet1)$, and the $\vec{\mathrm{p}}_{\mathrm{T}}$ of the Z boson, $\vec{\mathrm{p}}_{\mathrm{T}}(Z)$, are required to be back to back: $\Delta\phi(\vec{\mathrm{p}}_{\mathrm{T}}(jet1), \vec{\mathrm{p}}_{\mathrm{T}}(Z)) > 3.0$ rad.

Rarely the leading jet can be originating from another $p\overline{p}$ interaction produced in the same bunch crossing as the Z+jet; the overlapping jets biases $\mathrm{p_T}$-balance. The number of interactions in event is estimated via the number of primary vertices along the beam line; the number is used for the corresponding JES correction.

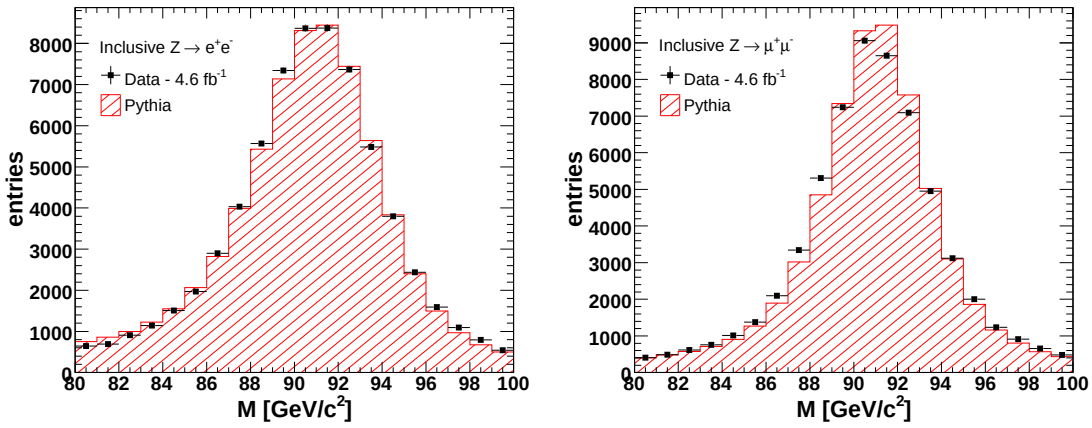

(a) (b)

Figure 1: The observed (points) and expected (histogram) distributions in the invariant mass of e^+e^- (a) and $\mu^+\mu^-$ (b) lepton pairs. The slight mismatch in data and Monte Carlo in the dimuon spectrum is due to a small miscalibration in the standard CDF tracking momentum scale.

The multiple interactions are mostly minimum bias events which produce relatively soft jets ($p_T \lesssim 8$ GeV/c).

We veto events with two or more primary vertices in which the leading jet is measured to come from a different interaction vertex than that of the hard interaction producing the Z-boson. The jet vertex of origin is determined using tracks pointing to the towers in the jet cluster. For each track we take z-coordinate of the point on the track closest to the beam-line. A mean value of the z-coordinates is calculated to determine the vertex of jet origin. Specifically, events are removed if the leading jet has two or more tracks, and the jet vertex is more than 2 cm away from the vertex of the lepton pair along the z-axis. The veto has a negligible effect on the p_T-balance as the leading jet p_T is required to be above 8 GeV/c.

We test the precision of the measurement of $p_T(Z)$ by using simulated events. In each event we find the average observed $p_T(Z)$ to be within 0.5% of the generated value. A distribution of the observed transverse momentum of Z-bosons, $p_T(Z)$, is shown in Fig. 2.

The Z-jet system is not a perfect two-body process and the p_T-balance, $p_T(jet1)/p_T(Z)$, is sensitive to the surroundings of the jet. Also, the jet energy resolution is rather poor (in comparison to the jet energy) for jets with p_T of about 10 GeV/c. The resolution improves with higher jet energies (it is about 20% for p_T(jet) = 40 GeV/c and 12% for p_T(jet) = 140 GeV/c). As an illustration that we can approach the ideal two-body system we apply a more stringent event selection; the p_T of sub-leading jets is required to be less than 3 GeV/c. The p_T-balance for the exclusive event selection is shown in Fig. 3. Distribution for events with $p_T(Z) < 25$ GeV/c is asymmetric and shifted from 1.0 due to the finite jet energy resolution and the cut-off on the minimum p_T of the leading jet (see Fig. 3 (a)). Distribution in p_T-balance for events

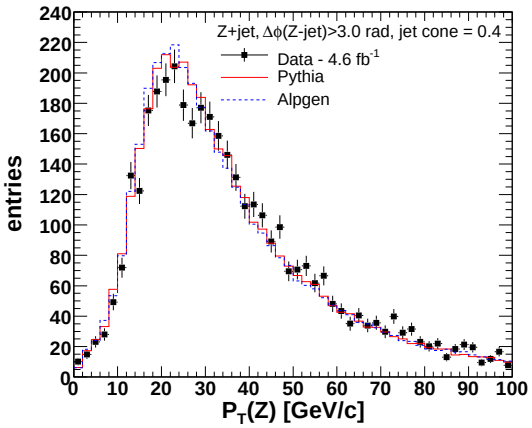

Figure 2: The observed (points) and expected (histogram) distributions in the transverse momentum of lepton pairs with invariant mass between 80< $M(\ell\ell)$ <100 GeV/c^2. The solid line is for the PYTHIA and the dashed line is for the ALPGEN predictions. All other sample selection cuts have been applied.

with $p_T(Z) > 25$ GeV/c is nearly symmetric and peaks close to 1.0 (see Fig. 3 (b)). Consequently we use events with $p_T(Z) > 25$ GeV/c to compare data and predictions. Further in the paper we will not use the 3 GeV/c cut-off on the sub-leading jet p_T as it was used to effectively prove the jet energy correction works properly. We will relax the cut-off to 8 GeV/c to better study the systematic uncertainties caused by the MC predictions.

6. Validation of SM simulations: Properties of quark and gluon jets

Properties of a QCD jet depend on the tree-level parton initiating it. A jet initiated by a gluon has a higher multiplicity of stable hadrons than a jet of the same energy initiated by a light quark. The difference in the observed particle multiplicities is due to the different color charges of quarks and gluons [28].

A quark jet deposits more energy in the calorimeter system on average than a gluon jet with the same true momentum. The difference is caused by the non-linear response of the calorimeter to single particles and the different multiplicities of hadrons. The predicted p_T-balances are presented as a function of $p_T(Z)$ for quark and gluon jets and for data in Figs. 4, 5, and 6 for the jet cone radii of 0.4, 0.7, and 1.0. The p_T-balance for quark jets is significantly different than that for gluon jets; it is consequently essential to check that the mixture of quark and gluon jets is predicted accurately by PYTHIA.

The fraction of quark and gluon jets in the Z-jet sample is largely driven by the parton distribution functions of the colliding particles (e.g. $p\bar{p}$ at the Tevatron and pp at the LHC) and the matrix elements of $q\bar{q} \to Zg$ and $qg \to Zq$ tree-level diagrams.

We test that the discrepancy in data vs. predictions (MC) in the p_T-balance is not caused by an

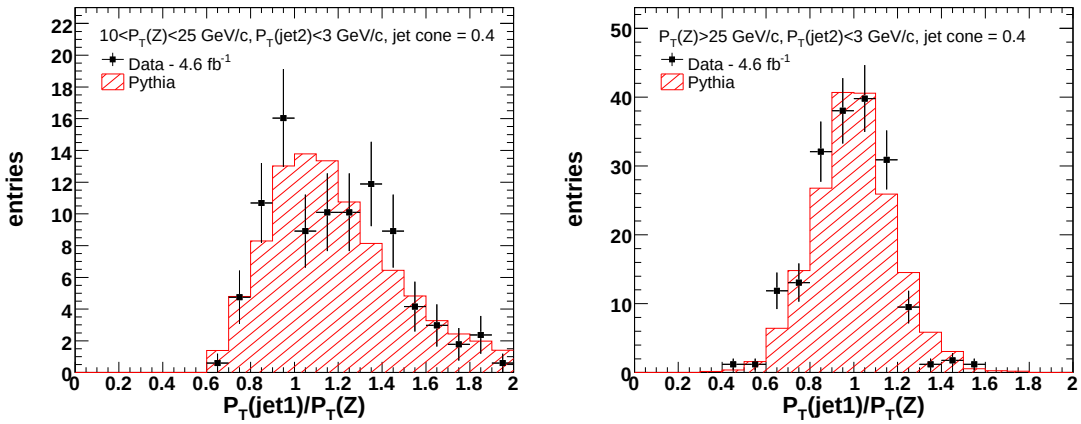

(a) (b)

Figure 3: The observed (points) and expected (histogram) distributions in p_T-balance, $p_T(jet1)/p_T(Z)$, for events with $p_T(Z)$ less than 25 GeV/c (a) and greater than 25 GeV/c (b). Sub-leading jets are required to have $p_T < 3$ GeV/c to suppress energy flow outside of the cone of the leading jet (see Section 5.1). The distribution (a), for $p_T(Z) < 25$ GeV/c, is noticeably distorted from a symmetric Gaussian shape due to a finite jet energy resolution and a cut-off on the minimum p_T of the leading jet.

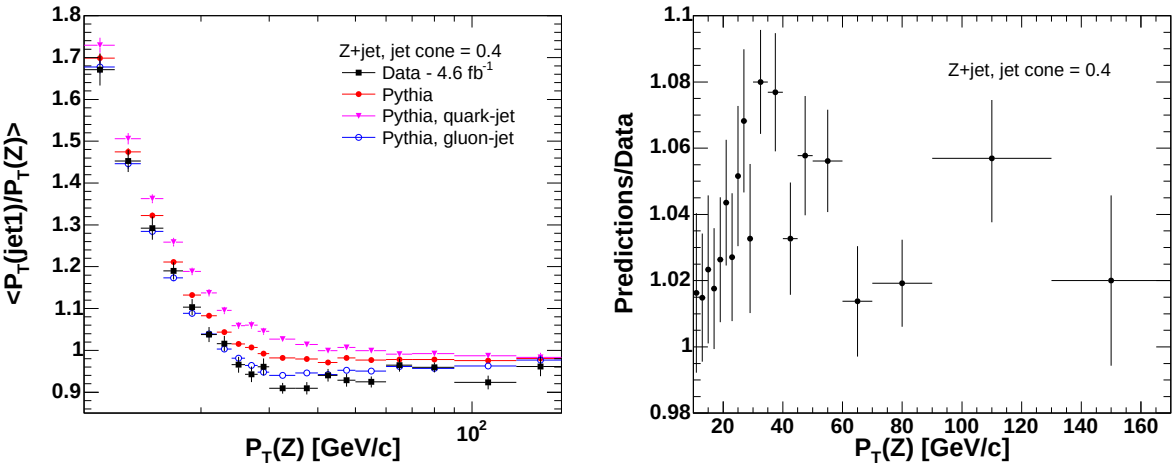

(a) (b)

Figure 4: a.) The average p_T-balance as a function of $p_T(Z)$. b.) The ratio of predicted and measured distributions in p_T-balance. The predicted distribution is for the combination of quark and gluon jets given by PYTHIA. The jets are clustered using a cone radius of R=0.4.

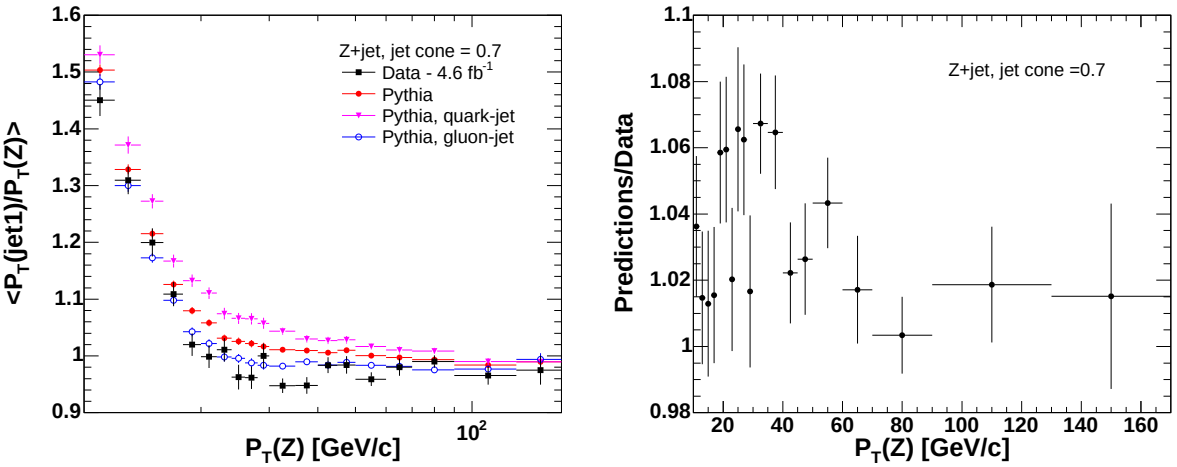

(a) (b)

Figure 5: a.) The average p_T-balance as a function of $p_T(Z)$. b.) The ratio of predicted and measured distributions in p_T-balance. The predicted distribution is for the combination of quark and gluon jets given by PYTHIA. The jets are clustered using a cone radius of R=0.7.

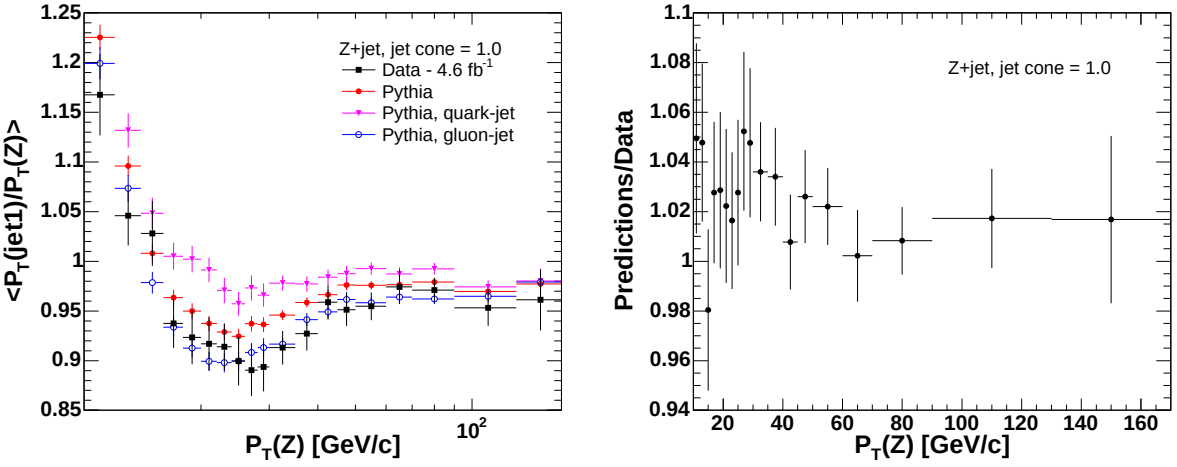

(a) (b)

Figure 6: a.) The average p_T-balance as a function of $p_T(Z)$. b.) The ratio of predicted and measured distributions in p_T-balance. The predicted distribution is for the combination of quark and gluon jets given by PYTHIA. The jets are clustered using a cone radius of R=1.0.

incorrectly modeled fraction of quark and gluon jets using two methods. We compare rapidity distributions for Z+jet events in Section 6.1 to validate the relative contributions from $qg \rightarrow Zq$ and $q\bar{q} \rightarrow Zg$ LO

diagrams in PYTHIA and ALPGEN. Having data, ALPGEN, and PYTHIA in good agreement, we further test the prediction from PYTHIA alone by looking at the number of tracks inside the jet cone (see Section 6.2).

The quark-gluon mixture is sensitive to PDFs, choice of renormalization and factorization scales, and LO matrix element for Z + 1-parton final state. The impact from those will be reported later in Sections 7, 8, 9, and 10.

6.1. Kinematic properties of Z+jet events

Kinematic properties of Z+jet events and quark/gluon composition of the leading jet both depend on the matrix elements and the PDFs. The kinematic properties thus indirectly probe the quark/gluon composition. The SM predictions are studied using the distributions of sum and difference of rapidities of a Z boson and the leading jet, $|y(Z)+\eta(jet1)|$ and $|y(Z)-\eta(jet1)|$, respectively (see Fig. 7). We require $p_T(Z) > 15$ GeV/c since the distributions are not sensitive to the jet energy resolution. We observe good agreement between data and the predictions (both ALPGEN and PYTHIA). The distributions are slightly different for ALPGEN and PYTHIA due to the different methods of computing MEs for the tree-level processes.

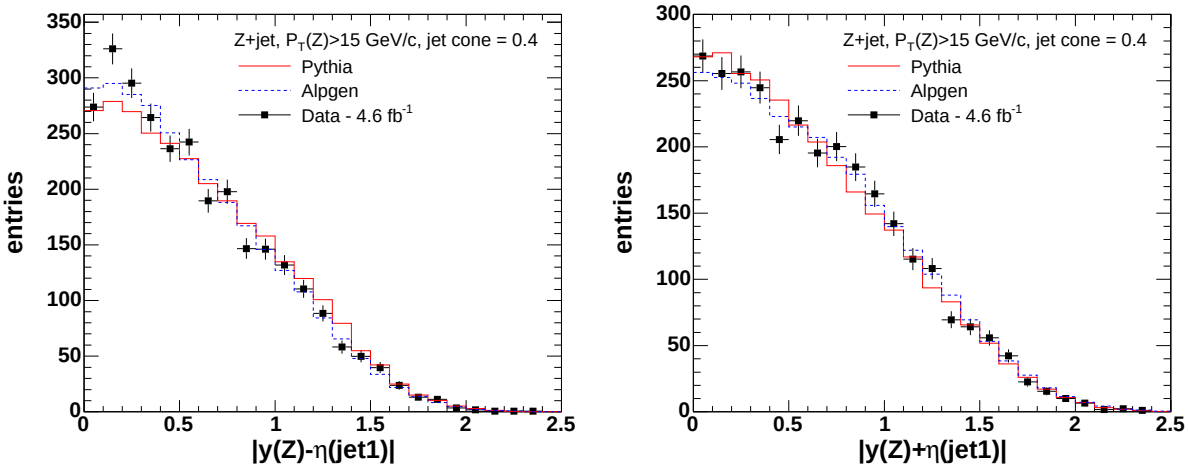

(a) (b)

Figure 7: The rapidity distributions for the Z+jet system. The jet clustering is performed with a cone of R=0.4.

6.2. Charged particle multiplicity in jets

We perform a direct test of the quark-gluon composition of the observed jets by using the number of tracks observed within the jet cone. The number of tracks is different for quark and gluon jets (see Fig. 8). Overall, the observed events are in good agreement with the SM predictions (PYTHIA).

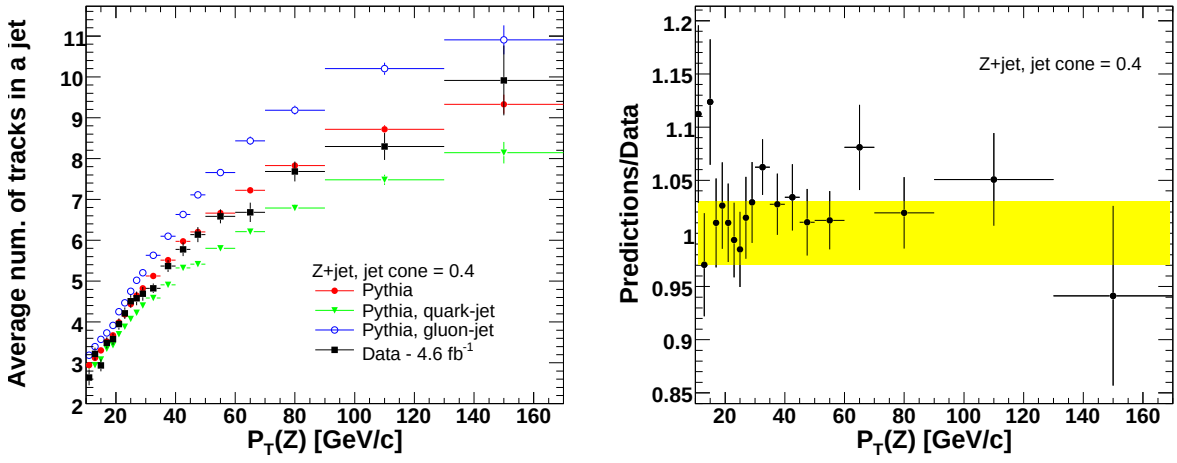

(a) (b)

Figure 8: a) The average number of tracks within a jet cone of radius of R=0.4 as a function of $p_T(Z)$. b) The ratio of the predicted number of tracks to the measured number in data versus $p_T(Z)$. The yellow band represents a 3% uncertainty on the predicted tracking efficiency [29].

We calculate the number of tracks reconstructed within the cone of the leading jet. The tracks are required to originate from the same vertex as the lepton pair forming a Z boson, $|z_0 - z_{track}| < 4$ cm and $|d_0(tracks)| < 0.02$ cm with SVX hits (0.2 cm without SVX). Also we require a good track quality for the tracks, namely χ^2 for the track fit divided by the number of degrees of freedom should be less than 6. The transverse momentum of the tracks is required to be greater than 0.3 GeV/c.

7. Uncertainty due to calculation of the matrix elements and the jet-parton matching scheme

Calculation of matrix elements (MEs) for Z+0 partons and Z+1 parton is different in ALPGEN+PYTHIA and stand-alone PYTHIA. In addition to that ALPGEN+PYTHIA simulation uses a veto algorithm to avoid double counting of jets produced by matrix elements and radiation from parton shower [6]. The difference in methods affects the p_T-balance obtained using the two event generators. We calculate the p_T-balance in both the ALPGEN and PYTHIA samples. The difference is found to be about 2-3% as shown in Table 1.

8. PDF uncertainties

We test the sensitivity of the p_T-balance to the choice of the PDF set used to generate events [30]. The default PDF set, CTEQ5L, is a single set of functions and it does not contain error functions. We estimate the PDF-related systematic uncertainty using the Hessian method; we take the CTEQ6M set, which includes

40 eigenvector error functions in addition to the central value. We re-weight the existing events with the parton densities provided by the CTEQ6M set. For each error set we calculate the difference in p_T-balance relative to the central value given by CTEQ6M. The sum in quadratures of the 40 variations in p_T-balance results in a negligibly small value (less that 0.1%) of the uncertainty on the predicted balance.

9. ISR uncertainties

In the Monte Carlo sample of inclusive Z events generated using PYTHIA, most of the jets arise from the ISR parton shower model (the underlying event model also contributes to production of soft jets), which depends upon several parameters that are not tightly constrained by data. As a result, the parameters of ISR affect the observed p_T-balance in Z+jet events.

To produce the systematics samples we altered the ISR settings used in PYTHIA, parameters PARP(61), PARP(64), and MSTP(3). Parameter MSTP(3) governs the choice of the Λ parameters used in the calculations of space-like (ISR) and time-like (FSR) parton showers. The parameter Λ is used in running of α_s. By default when MSTP(3) is 2, the value of Λ is chosen according to the PDF parameterizations. We set MSTP(3) to 1 to overwrite the value of PARP(61), which defines Λ used in space-like parton showers. Parameter PARP(64) is also used in the calculation of α_s and parton distributions as a multiplier for the squared transverse momentum evolution scale, $k_\perp^2$.

The variations in p_T-balance calculated for the systematics samples relative to the default one are used to estimate the ISR uncertainty. The resulting value is on the order of 1%.

10. Uncertainty due to renormalization and factorization scales

Predictions for Z+jet production are sensitive to the choice of renormalization and factorization scales. The accuracy of LO calculations is often estimated by varying renormalization and factorization scales (NLO calculations demonstrate weaker dependence on the scales) [31]. The scales impact calculation of the LO matrix elements for events with a Z boson and N partons. We exploit ALPGEN to generate events with altered renormalization and factorization scales. The scales are always kept the same by ALPGEN, with a default value is $Q_0 = \sqrt{M_Z^2 + \Sigma p_T^2(jet)}$. We produce two "systematic" samples with Q_0 being multiplied by 0.5 or 2.0. The choice of the scales impacts the predicted p_T-balance by up to 1-2% as recorded in Table 1.

The effect due to variation of renormalization and factorization scales in ALPGEN is similar to that caused by variation of the ISR parameters in PYTHIA (see Sec. 9). The stand-alone PYTHIA method of calculations for the inclusive production of Z bosons uses an ISR parton shower to estimate the LO matrix element for Z plus one parton. Both methods deal with the same computational uncertainty caused by limited accuracy of the LO calculations used in the two MC event generators so that the variation of scales results in similar

uncertainties for the both generators. We use the variation in p_T-balance estimated with ALPGEN and not that obtained with PYTHIA to avoid double-counting the effect.

11. Characteristics of out-of-cone radiation

An understanding of the energy flow outside of the cone of the leading jet is essential for interpreting the measurement of p_T-balance in Z-jet events. Raw calorimeter energy summed in annuli outside of the jet cone is not linearly proportional to the true out-of-cone energy.

We exploit correlations between p_T-balance and properties of the sub-leading jet such as p_T(jet2) and $\Delta\phi(jet1-jet2)$. Multiple $p\overline{p}$ interactions produce additional soft jets which are unrelated to the jets recoiling against the Z-boson. The presence of additional interactions might bias the correlation between the p_T-balance and the properties of the sub-leading jet. In the method described in this section we require all events to have exactly one primary vertex, one interaction. The requirement to have exactly one primary vertex was not applied before since we did not have to measure jet clusters with p_T softer than 8 GeV/c.

We measure the dependence of the p_T-balance on the azimuthal angle between the leading jet ($jet1$) and the sub-leading one ($jet2$), $\Delta\phi(jet1 - jet2)$, for events with $p_T(Z) > 25$ GeV/c (see Figs. 9, 10, and 11). The observed dependence of the p_T-balance on the angular separation between the 1st and the 2nd jets is sensitive to the jet cone size. As expected the largest discrepancy between data and the predictions is observed with the smallest jet cone size of R=0.4 (see Fig. 9), for which the particle-jet-energy to parton-jet-energy correction is at maximum. Larger jet cone sizes give result in better agreement between data and PYTHIA simulations. Two cone 0.4 jets can be reconstructed as one cone-1.0 jet. As a result the large-angle radiation most likely falls within the jet cone of R=1.0.

The positive correlation between the p_T-balance and $\Delta\phi(jet1 - jet2)$ shows that the 2nd jet is often caused by the parton radiation from the leading jet as the magnitude of the correlation is proportional to the rate of the large-angle parton radiation. Positive slope of the ratio between data and predictions (e.g. see Fig. 9(b)) indicates that the data exhibit more large-angle parton radiation than the MC simulations. The deficiency of large-angle parton radiation is also consistent with the results from [32].

We measure the dependence of the p_T-balance on the p_T of the second jet, p_T(jet2). The balance as a function of the 2nd jet p_T is shown in Figs. 12, 13, and 14 for different sizes of jet cones. The balance is the most sensitive to the 2nd jet p_T when the jet cone is 0.4 (see Fig. 12). The observed rate of large-angle out-of-cone radiation is also observed to be higher in data than in the predictions.

11.1. Uncertainty due to out-of-cone radiation

We use the p_T-cutoff of the sub-leading jet to estimate the variation of the balance due to the out-of-cone radiation. The agreement between data and predictions improves as we decrease the cut-off value on

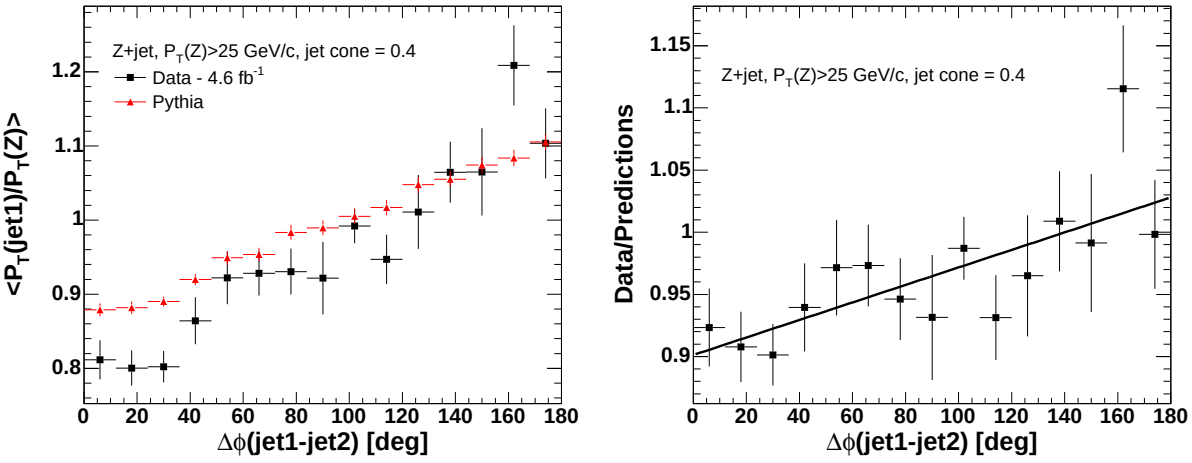

(a) (b)

Figure 9: a.) A comparison of the measured (square markers) and predicted (triangle markers) p_T-balance as a function of $\Delta\phi(jet1-jet2)$ for jets of R=0.4 cone size. The predicted balance is obtained with PYTHIA. The events are required to have an only one interaction per event. b.) The fit of the ratio to a line results in $\chi^2/NDF = 10.0/14$ and slope $= 7.05{\cdot}10^{-4} \pm 1.84{\cdot}10^{-4}$, as could be explained by an inadequate modeling of large-angle parton radiation.

$p_T(jet2)$ as shown in Figs. 12, 13, and 14 (all the other selection requirements are kept the same). The extrapolation to the point where $p_T(jet2)$ is zero describes the case where both data and predictions do not have any large-angle FSR.

We take the variation of the ratio of p_T-balance between data and prediction as an estimate of the uncertainty due to large angle FSR. The ratio is obtained as a function of p_T of the sub-leading jet, $p_T(jet2)$. The difference between ratios for $p_T(jet2) \to 0$ GeV/c (we obtain that using the linear extrapolation) and $p_T(jet2) < 8$ GeV/c is taken as a systematic uncertainty. The obtained uncertainties are summarized in Table 1.

12. Final state radiation uncertainties

Final state radiation (FSR) from unfragmented partons is modeled by time-like parton showers in PYTHIA. The predicted p_T-balance is sensitive to the rate of FSR. In this study, the variation of FSR parameters is performed similarly to that for ISR (see Section 9). To produce the systematics samples we altered the parameters PARP(72), PARP(71), and MSTP(3) in PYTHIA. The value of PARP(72) defines the QCD parameter Λ used in simulation of time-like showers of partons produced in ISR. By default, the Lambda parameter of the PDF set (CTEQ5L in this case) is used for ISR (PARP(61)) and FSR of ISR partons

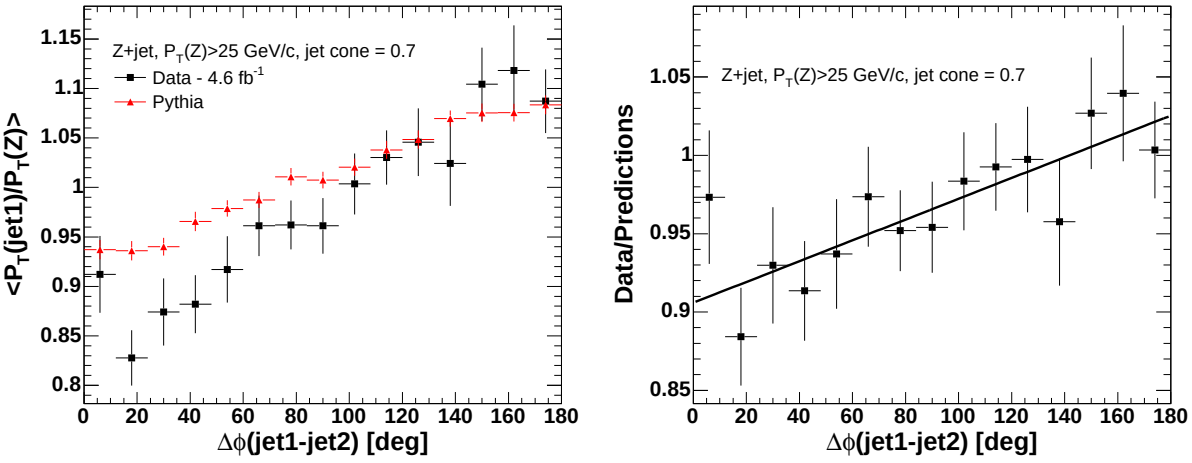

(a) (b)

Figure 10: a.) A comparison of the measured (square markers) and predicted (triangle markers) p_T-balance as a function of $\Delta\phi(jet1 - jet2)$ for jets of R=0.7 cone size. The predicted balance is obtained with PYTHIA The events are required to have an only one interaction per event. b.) The fit of the ratio to a line results in $\chi^2/NDF = 6.9/14$ and slope $= 6.6{\cdot}10^{-4} \pm 1.8{\cdot}10^{-4}$.

(PARP(72)). The value of PARP(71) is used as a multiplicative scaling factor to the Q^2 scale of the hard scattering to define the maximum parton virtuality for time-like showers. The variation of p_T-balance in the FSR systematics samples is about 1% as shown in Table 1.

13. Multiple proton-proton interactions

The p_T-balance is sensitive to multiple $p\overline{p}$ interactions overlapping in-time with the hard process ("pile-up"). The number of interactions per event is estimated by observing additional primary vertices along the beam-line. The additional interactions are likely to be minimum-bias collisions.

The uncertainty in the p_T-balance arises from the present limited ability to measure accurately the calorimeter energy in a minimum bias event. The momentum distribution of charged particles in the predictions, measured in the magnetic spectrometer (COT), was tuned to data only for particles with $p_T >$ 0.5 GeV/c [33] as soft charged particles ($p_T <$ 0.3 GeV/c) curl up in the magnetic field and do not reach the calorimeters. Consequently the response for soft ($p_T <$ 0.5) neutral hadrons is not measured. The difference between data and prediction, on the order of a percent, is taken as a systematic uncertainty (see Table 1).

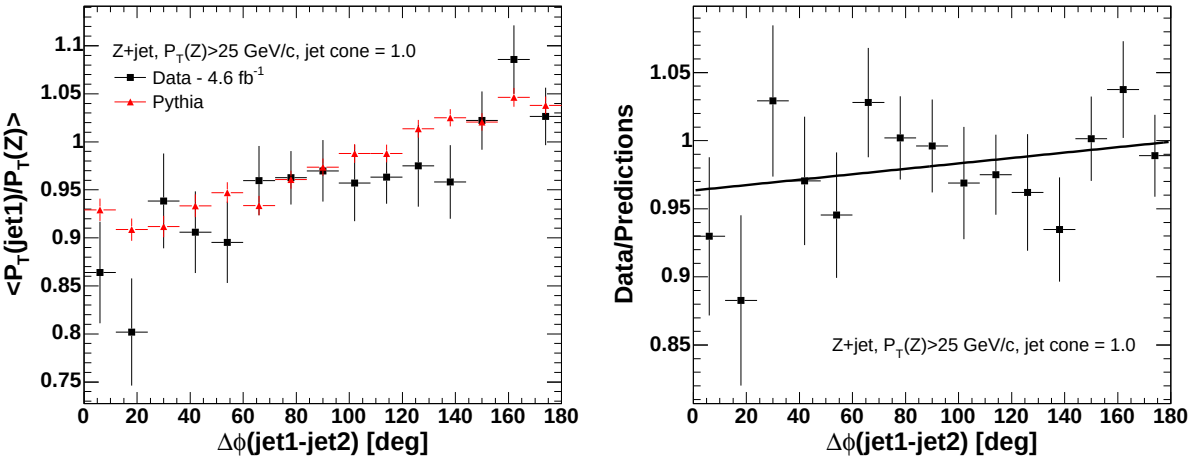

(a) (b)

Figure 11: a.) A comparison of the measured (square markers) and predicted (triangle markers) p_T-balance as a function of $\Delta\phi(jet1 - jet2)$ for jets of R=1.0 cone size. The predicted balance is obtained with PYTHIA. The events are required to have an only one interaction per event. b.) The fit of the ratio to a line results in $\chi^2/NDF = 10.5/14$ and slope $= 2.0{\cdot}10^{-4} \pm 2.1{\cdot}10^{-4}$.

14. Detector simulations for single particle response

The jet energy scale is based on measurements of the response of the calorimeters to single charged particles whose momenta are measured precisely using the magnetic spectrometer of CDF as well as test-beam measurements at the highest momenta [2]. Uncertainties in transferring the measured single-particle response to a parametric model of the calorimeter jet response contribute significantly to the uncertainty on the CDF jet-energy-scale. We vary the single particle response in PYTHIA sample by $\pm 1\sigma$ to estimate its effect on the p_T-balance. The contributions are typically 2.5% (see Table 1).

15. Summary of systematic uncertainties

We observe a significant discrepancy in the p_T-balance of Z-bosons and single jets between measurements and prediction, with the data being lower in the p_T of the jet compared to predictions. In Table 1 we summarize the estimated variations (taken as systematic uncertainties) of the predicted balance. The totality of the variations is comparable to the observed discrepancy, with the largest contributions being those from large-angle FSR and the modeling of the single-particle response of the calorimeters.

Data indicates that the large-angle parton radiation is not modeled accurately by the leading-log parton showering from PYTHIA Tune AW: the MC simulation underestimates the large-angle radiation. The dis-

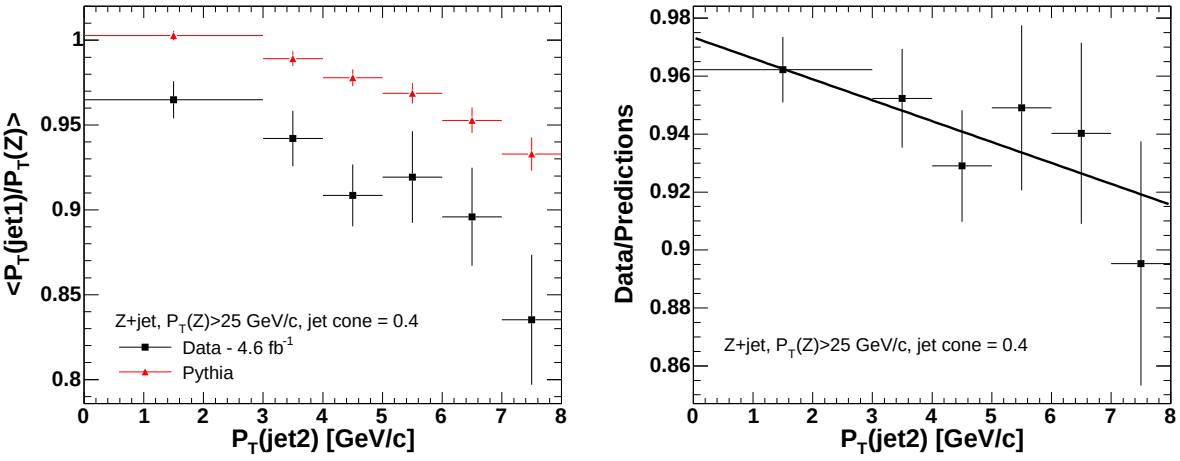

(a) (b)

Figure 12: a.) A comparison of the measured (square makers) and predicted (triangle markers) p_T-balance as a function of the 2nd jet p_T for jets of R=0.4 cone size. The predicted balance is obtained with PYTHIA. The events are required to have only one interaction per event. b.) The ratio of predicted to measured p_T-balance versus the p_T of the second jet. The linear fit of the ratio resulted in a slope of -0.7±0.4 %/ GeV/c.

crepancy is not addressed by the predictions from ALPGEN + PYTHIA either; the ME calculations affect only jets with p_T above the matching scale (15 GeV/c in the analysis); softer radiation (p_T(jet2) $<$ 8 GeV/c in the analysis) is simulated via the parton showering mechanism.

16. Conclusions

We have estimated the sensitivity of the predicted p_T-balance to the virtuality-ordered parton showering from PYTHIA, tree-level matrix elements, parton distribution functions, parton-jet matching procedure, renormalization and factorization scales, multiple $p\overline{p}$ interactions, and calorimeter response of single stable particles. The contribution from each source of uncertainty is presented in Table 1. The uncertainty caused by inadequate modeling of the parton shower at large angles is found to be the largest. The sum of the uncertainties is consistent with the discrepancy between data and predictions in the p_T-balance. The remaining uncertainties are significantly smaller [2].

Numerous modern higher-order MC simulations utilize leading-log parton showering from PYTHIA [34, 35]. The higher-order calculations of the matrix elements are less sensitive to the choice of renormalization and factorization scales so that the related uncertainty should be smaller than that we evaluated. However, the uncertainty due to large-angle parton radiation is expected to be of the same magnitude as in the study.

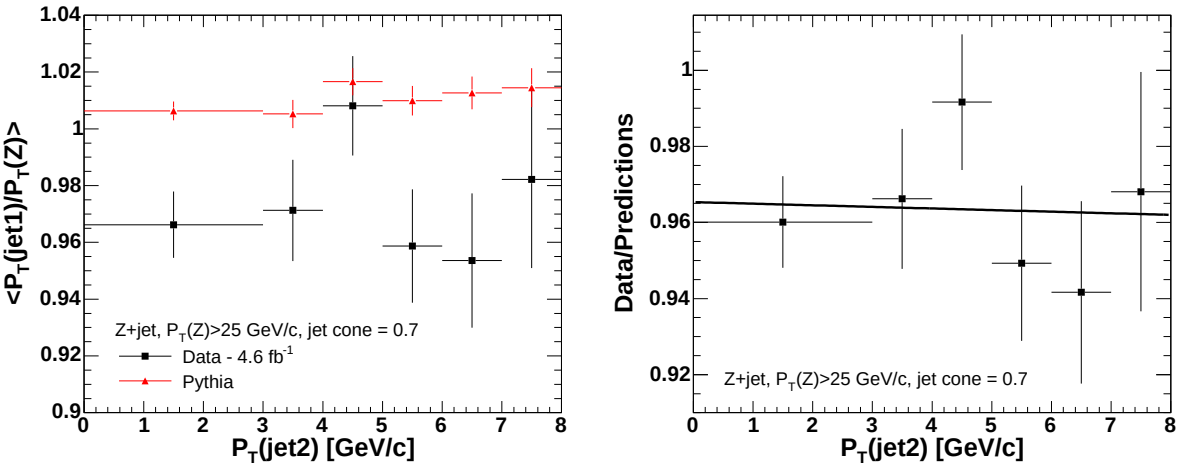

(a) (b)

Figure 13: a.) A comparison of the measured (square markers) and predicted (triangle markers) p_T-balance as a function of the 2nd jet p_T for jets of R=0.7 cone size. The predicted balance is obtained with PYTHIA. The events are required to have only one interaction per event. b.) The ratio of predicted to measured p_T-balance versus the p_T of the second jet. The linear fit of the ratio resulted in a slope of -0.04±0.04 %/ GeV/c.

We suggest that the LHC experiments should use the distributions in Figs. 9, 10, 11 and 12, 13, 14 as a systematic method for tuning the parton showing parameters in event generators for more accurate jet energy measurements.

Acknowledgments

We thank the Fermilab staff and the technical staffs of the participating institutions for their vital contributions. This work was supported by the U.S. Department of Energy and National Science Foundation; the Italian Istituto Nazionale di Fisica Nucleare; the Ministry of Education, Culture, Sports, Science and Technology of Japan; the Natural Sciences and Engineering Research Council of Canada; the National Science Council of the Republic of China; the Swiss National Science Foundation; the A.P. Sloan Foundation; the Bundesministerium für Bildung und Forschung, Germany; the World Class University Program, the National Research Foundation of Korea; the Science and Technology Facilities Council and the Royal Society, UK; the Institut National de Physique Nucleaire et Physique des Particules/CNRS; the Russian Foundation for Basic Research; the Ministerio de Ciencia e Innovación, and Programa Consolider-Ingenio 2010, Spain; the Slovak R&D Agency; and the Academy of Finland. This work has also been supported by the Maria Goeppert Meyer Fellowship of Argonne National Laboratory, NSF, and DOE.

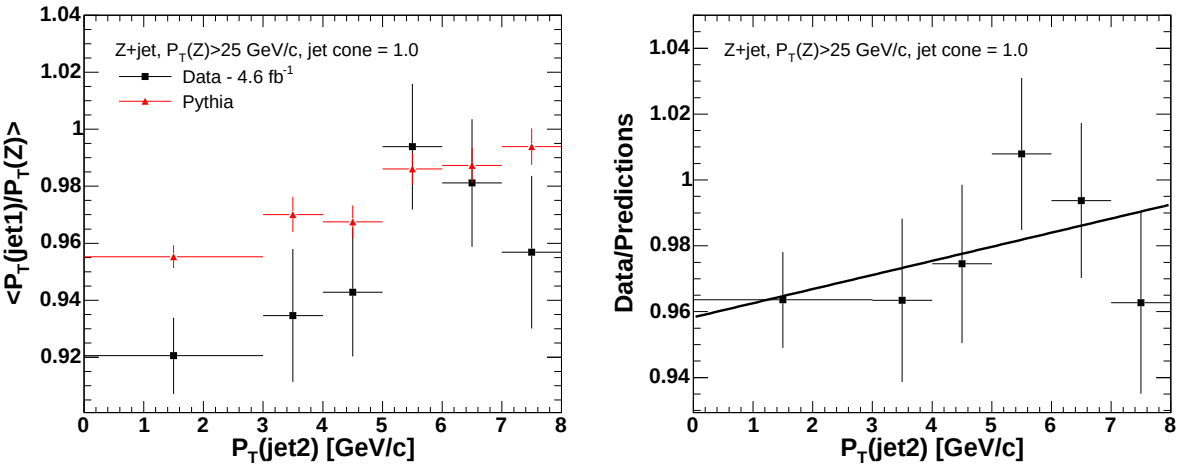

(a) (b)

Figure 14: a.) A comparison of the measured (square markers) and predicted (triangle markers) p_T-balance as a function of the 2nd jet p_T for jets of R=1.0 cone size. The predicted balance is obtained with PYTHIA. The events are required to have only one interaction per event. b.) The ratio of predicted to measured p_T-balance versus the p_T of the second jet. The linear fit of the ratio resulted in a slope of 0.4±0.4 %/ GeV/c.

We are thankful to David Mietlicki, Ray Culbertson, Peter Skands, Torbjorn Sjostrand, Alexander Pronko, Larry Nodulman, Willis Sakumoto, Michelangelo Mangano, Christina Mesropian, Eric J. Feng, and Jan-Christopher Winter for suggestions.

References

[1] B. Meirose, Determination of QCD Backgrounds in ATLAS: A challenge for SUSY searches (2009).

[2] A. Bhatti, et al., Determination of the jet energy scale at the collider detector at fermilab, Nucl. Instrum. Meth. A 566 (2006) 375–412.

[3] B. Abbott, et al., Determination of the absolute jet energy scale in the DØ calorimeters, Nucl. Instrum. Meth. A424 (1999) 352–394.

[4] T. Sjostrand, L. Lonnblad, S. Mrenna, Pythia 6.2: Physics and manual (2001).

[5] M. L. Mangano, M. Moretti, F. Piccinini, R. Pittau, A. D. Polosa, Alpgen, a generator for hard multiparton processes in hadronic collisions, JHEP 0307 (2003) 001.

[6] M. L. Mangano, M. Moretti, F. Piccinini, M. Treccani, Matching matrix elements and shower evolution for top-quark production in hadronic collisions, JHEP 01 (2007) 013.

[7] ???? The CDF-II detector is described in more detail in many recent publications; see, for example, A. Abulencia et al., (CDF Collaboration), Phys. Rev. D **73**, 112006 (2006), and references therein.

[8] ???? Transverse momentum and energy are defined as $p_T = p \sin\theta$ and $E_T = E \sin\theta$, respectively.

[9] ???? A. Sill et al., Nucl. Instrum. Meth. A **447**, 1 (2000); A. Affolder et al., Nucl. Instrum. Meth. A **453**, 84 (2000); C.S. Hill, Nucl. Instrum. Meth. A **530**, 1 (2000).

Source of uncertainty	R = 0.4	R = 0.7	R = 1.0
renormalization and factorization scales	+0.9 -0.0	+0.9 -0.4	±0.4
FSR parameters in PYTHIA	±0.4	±0.1	±0.1
MEs and parton-jet matching	+0.8 -0.0	+1.1 -0.0	+0.8 -0.0
single particle response	±2.5	±2.5	±2.5
multiple proton interactions	+1.0 -0.0	+1.2 -0.0	+1.2 -0.0
large-angle FSR, limitation of PS	+0.0 -2.9	+0.0 -0.2	+1.7 -0.0
Estimate of the total variation	+3.0 -3.8	+3.1 -2.5	+3.4 -2.5
The observed discrepancy	+4.7	+3.2	+2.0

Table 1: The effect on the predicted mean p_T-balance of varying parameters in the modeling and event selection, in percent, for jet cone sizes R = 0.4, 0.7, and 1.0. The variations are evaluated for PYTHIA events with $p_T(Z) > 25$ GeV/c. The observed discrepancy is defined as the p_T-balance in predictions divided by that in data; the predicted jet energies are higher than those in data. The discrepancy between data and predictions is comparable with the estimate of the total variation of the predictions. A positive variation in the predicted p_T-balance corresponds to an increase in the jet energies in the MC predictions. The total variation is calculated by adding the uncertainties in quadrature.

[10] ???? The CDF coordinate system is cylindrical and right-handed, with the x axis horizontal and out of the Tevatron ring, the y axis up, the z axis along the proton beam, and $r = \sqrt{x^2 + y^2}$; ϕ is the azimuthal angle. The pseudorapidity $\eta \equiv -\ln(\tan(\theta/2))$, where θ is the polar angle; the η regions for detector components are defined with respect to the center of the detector. The central region is defined as $|\eta| < 1$.

[11] ???? A. Affolder et al., Nucl. Instrum. Meth. A **526**, 249 (2004).

[12] T. Aaltonen, et al., First run ii measurement of the w boson mass at the fermilab tevatron, Phys. Rev. D 77 (2008) 112001.

[13] ???? L. Balka et al., Nucl. Instrum. Meth. A **267**, 272 (1988).

[14] ???? S. Kuhlmann et al., Nucl. Instrum. Meth. A **518**, 39 (2004).

[15] G. Apollinari, K. Goulianos, P. Melese, M. Lindgren, Shower maximum detector for the cdf plug upgrade calorimeter, Nuclear Instruments and Methods in Physics Research Section A: Accelerators, Spectrometers, Detectors and Associated Equipment 412 (1998) 515 – 526.

[16] ???? D. Acosta et al. (CDF Collaboration), Phys. Rev. D **71**, 032001 (2005).

[17] ???? M. G. Albrow et al. (CDF Collaboration), Nucl. Instrum. Meth. A **480**, 524 (2002).

[18] ???? G. Ascoli et al. (CDF Collaboration), Nucl. Instrum. Meth. A **268**, 33 (1988).

[19] ???? T. Dorigo et al. (CDF Collaboration), Nucl. Instrum. Meth. A **461**, 560 (2001).

[20] ???? D. Acosta et al. (CDF Collaboration), Nucl. Instrum. Meth. A **494**, 57 (2002).

[21] D. Acosta, et al., First measurements of inclusive w and z cross sections from run ii of the tevatron collider, Phys. Rev. Lett. 94 (2005) 091803.

[22] R. Field, Jet physics and the underlying event at the Tevatron, AIP Conf. Proc. 828 (2006) 163–174. We use Tune A.

[23] T. Aaltonen, et al., Measurement of the k_T Distribution of Particles in Jets Produced in $p\bar{p}$ Collisions at $\sqrt{s} = 1.96$-TeV,

Phys. Rev. Lett. 102 (2009) 232002.

[24] D. Acosta, T. Affolder, H. Akimoto, et al., Momentum distribution of charged particles in jets in dijet events in $p\bar{p}$ collisions at $\sqrt{s}$=1.8 tev and comparisons to perturbative qcd predictions, Phys. Rev. D 68 (2003) 012003.

[25] D. Acosta, J. Adelman, T. Affolder, T. Akimoto, M. G. Albrow, D. Ambrose, S. Amerio, D. Amidei, A. Anastassov, K. Anikeev, A. Annovi, J. Antos, M. Aoki, G. Apollinari, T. Arisawa, J.-F. Arguin, A. Artikov, W. Ashmanskas, A. Attal, F. Azfar, P. Azzi-Bacchetta, N. Bacchetta, H. Bachacou, W. Badgett, A. Barbaro-Galtieri, G. J. Barker, V. E. Barnes, Study of jet shapes in inclusive jet production in $p\overline{p}$ collisions at $\sqrt{s} = 1.96$ TeV, Phys. Rev. D 71 (2005) 112002.

[26] T. Aaltonen, J. Adelman, T. Akimoto, M. G. Albrow, et al., Global search for new physics with $2.0fb - 1$ at cdf, Phys. Rev. D 79 (2009) 011101.

[27] F. Abe, et al., Topology of three-jet events in $p\bar{p}$ collisions at $\sqrt{s}$=1.8 tev, Phys. Rev. D 45 (1992) 1448–1458.

[28] M. Derrick, K. K. Gan, P. Kooijman, J. S. Loos, B. Musgrave, L. E. Price, J. Schlereth, K. Sugano, J. M. Weiss, D. E. Wood, D. Blockus, B. Brabson, S. W. Gray, C. Jung, H. Neal, H. Ogren, D. R. Rust, M. Valdata-Nappi, C. Akerlof, G. Bonvicini, J. Chapman, D. Errede, N. Harnew, P. Kesten, D. I. Meyer, D. Nitz, A. A. Seidl, R. Thun, T. Trinko, M. Willutzky, S. Abachi, P. Baringer, I. Beltrami, B. G. Bylsma, R. Debonte, D. Koltick, F. J. Loeffler, E. H. Low, R. L. McIlwain, D. H. Miller, C. R. Ng, L. K. Rangan, E. I. Shibata, B. Cork, Comparison of charged particle multiplicities in quark and gluon jets produced in e+e- annihilation at 29 gev, Physics Letters B 165 (1985) 449 – 453.

[29] T. Aaltonen, et al., Measurement of Cross Sections for b Jet Production in Events with a Z Boson in p^- anti-p Collisions at $\sqrt{s} = 1.96$-TeV, Phys. Rev. D79 (2009) 052008.

[30] J. Pumplin, et al., New generation of parton distributions with uncertainties from global QCD analysis, JHEP 07 (2002) 012.

[31] V. Barger, T. Han, J. Ohnemus, D. Zeppenfeld, Perturbative qcd calculations of weak-boson production in association with jets at hadron colliders, Phys. Rev. D 40 (1989) 2888–2897.

[32] V. M. Abazov, et al., Measurement of $Z/\gamma^* + jet + X$ angular distributions in $p\bar{p}$ collisions at $\sqrt{s} = 1.96$ TeV, Phys. Lett. B682 (2010) 370–380.

[33] T. Affolder, H. Akimoto, A. Akopian, et al., Charged jet evolution and the underlying event in proton-antiproton collisions at 1.8 tev, Phys. Rev. D 65 (2002) 092002.

[34] K. Hamilton, P. Nason, Improving NLO-parton shower matched simulations with higher order matrix elements (2010).

[35] P. Torrielli, S. Frixione, Matching NLO QCD computations with PYTHIA using MC@NLO, JHEP 04 (2010) 110.

[36] A. Abulencia, et al., Measurements of Inclusive W and Z Cross Sections in p-pbar Collisions at sqrts =1.96 TeV, J. Phys. G34 (2007) 2457–2544.

[37] ???? For central electrons at least 5 hits in each of 3 axial and 2 stereo layers of the COT are required.

[38] ???? The fraction of electromagnetic energy allowed to leak into the hadron compartment $\mathrm{E_{had}/E_{em}}$ must be less than $0.055 + 0.00045 \times \mathrm{E_{em}(GeV)}$ for central electrons, less than 0.05 for electrons in the end-plug calorimeters, less than max[0.125, $0.055 + 0.00045 \times \mathrm{E_{em}(GeV)}$] for photons.

[39] ???? D. Acosta et al. (CDF Collaboration), Phys. Rev. D **71**, 051104 (2005); hep-ex/0501023.

[40] ????. For tight muons at least 5 hits in each of 3 axial and 3 stereo layers of the COT are required; for loose muons with a matching muon stub this is relaxed to 3 axial and 2 stereo. Loose muons without a matching stub have an additional cut on the χ^2 for the fit to the track.

[41] ????. The energy deposited in the calorimeter tower traversed by the muon must be less than $2 + \max(0, 0.0115 \times (p - 100))$ GeV in the electromagnetic compartment and less than $6 + \max(0, 0.028 \times (p - 100))$ GeV in the hadronic compartment.

[42] A. V. Varganov, The Production Cross Sections of the Weak Vector Bosons in Proton Antiproton Collisions at $\sqrt{s} =$ 1.96 TeV and a Measurement of the W Boson Decay Width. , Ph.D. thesis, University of Michigan, 2004. FERMILAB-THESIS-2004-39.

[43] ???? The muon "stub" in the muon systems must be within 7, 5, and 6 cm of the extrapolated COT track position, in the CMU, CMP, and CMX muon systems, respectively.
[44] A. V. Kotwal, H. K. Gerberich, C.Hays, Identification of cosmic rays using drift chamber hit timing, Nucl. Instrum. Meth. A 506 (2003) 110 – 118.
[45] ???? The maximum correction to the identification efficiency for central electrons is 1.7%, for "plug" electrons 6.3%, and for central muons is 7.4%.
[46] T. Aaltonen, A. Abulencia, J. Adelman, et al., First run ii measurement of the w boson mass at the fermilab tevatron, Phys. Rev. D 77 (2008) 112001.

Appendix A. Lepton identification

We use standard CDF definitions for identification (ID) of electrons and muons as described below [36]. The same lepton ID requirements are applied to events from data and Monte Carlo simulations.

The identification and triggering efficiencies for leptons are different for events in data and Monte Carlo, although they demonstrate a very similar energy dependence. To eliminate this inconsistency we follow the standard CDF practice of using correction factors ("scale factors") to re-weight the MC events (see Section Appendix A.3).

In order to maintain a high efficiency for Z bosons, for which we require two identified leptons, we define "tight" and "loose" selection criteria for both electrons and muons, as described below.

To reduce backgrounds from the decays of hadrons produced in jets, leptons are required to be "isolated". The $E_{\rm T}$ deposited in the calorimeter towers in a cone in $\eta-\varphi$ space [10] of radius $R = 0.4$ around the lepton position is summed, and the $E_{\rm T}$ due to the lepton is subtracted. The remaining $E_{\rm T}$ is required to be less than 10% of the lepton $E_{\rm T}$ for electrons or $\rm p_T$ for muons.

Appendix A.1. Electron selection

An electron candidate passing the "tight" selection must be central with $E_{\rm T} > 20$ GeV, and have: a) a high quality track [37] with $\rm p_T > 0.5 \cdot E_T$ or $\rm p_T > 50$ GeV/c; b) a good transverse shower profile at shower maximum that matches the extrapolated track position; c) a lateral sharing of energy in the two calorimeter towers containing the electron shower consistent with that expected; and d) minimal leakage into the hadron calorimeter [38].

Additional central electrons, classified as "loose" electrons, are required to satisfy the "tight" central electron criteria but with a track requirement of $\rm p_T > 10$ GeV/c (rather than $0.5 \cdot E_{\rm T}$), and no requirement on a shower maximum measurement or lateral energy sharing between calorimeter towers. Electrons in the forward calorimeters ($1.2 < |\eta| < 2.5$), also classified as "loose" electrons, are required to have $E_{\rm T} > 20$ GeV, minimal leakage into the hadron calorimeter, a track containing at least 3 hits in the silicon tracking system, and a shower transverse shape consistent with that expected, with a centroid close to the extrapolated position of the track [39].

Appendix A.2. Muon selection

A muon candidate passing the tight cuts must have: a) a well measured track in the COT [40] with $p_T > 20$ GeV/c; b) energy deposited in the calorimeter consistent with expectations [41]; c) a muon "stub" [42] in both the CMU and CMP, or in the CMX, consistent with the extrapolated COT track [43]; and d) a COT track fit consistent with an outgoing particle from a $p\overline{p}$ collision and not from an incoming cosmic ray [44].

Additional muons, classified as "loose", are required to have $p_T > 20$ GeV/c and to satisfy the same criteria as for tight muons but with relaxed COT track quality requirements. Alternatively, for muons outside the muon system fiducial volume, a loose muon must satisfy the tight muon criteria and an additional more stringent requirement on track quality, but the requirement that there be a matching "stub" in the muon systems is dropped.

Appendix A.3. Corrections due to Modeling of Electrons and Muons

Following the standard treatment of lepton efficiencies in CDF, we re-weight Monte Carlo events to take into account the difference between the identification efficiencies measured in leptonic Z decays and those used in simulation [45]. We then make additional corrections for the difference in trigger efficiencies in simulated events and measured in data. Corrections to trigger efficiencies are typically 4% for trigger electrons, 8% for trigger muons that traverse both the CMU and CMP systems, and 5% for muons in the CMX system. The average weight for $Z \to e^+e^-$ events is 0.939; for $Z \to \mu^+\mu^-$ events it is 0.891.

We correct the energy of electrons and muons the same way as it was done for the measurement of the W boson mass [46]. The relative positions of the tracker wires were aligned using cosmic muons. Additional track-level corrections were derived using $W \to e\nu$ data to reduce bias between positive and negative particles. The electron energy was corrected in data for effects due to tower position and time (aging).